HHS Public Access

Author manuscript

Matter. Author manuscript; available in PMC 2021 April 01.

Published in final edited form as:

Matter. 2020 April 1; 2(4): 921–937. doi:10.1016/j.matt.2020.01.021.

Investigation of cortisol dynamics in human sweat using a graphene-based wireless mHealth system

Rebeca M. Torrente-Rodríguez[1,3], **Jiaobing Tu**[1,3], **Yiran Yang**[1], **Jihong Min**[1], **Minqiang Wang**[1], **Yu Song**[1], **You Yu**[1], **Changhao Xu**[1], **Cui Ye**[1], **Waguih William IsHak**[2], **Wei Gao**[1,4,*]

[1]Department of Medical Engineering, Division of Engineering and Applied Science, California Institute of Technology, Pasadena, California, 91125, USA

[2]Department of Psychiatry and Behavioral Neurosciences, Cedars-Sinai Medical Center, Los Angeles, CA 90048, USA

[3]These authors contributed equally to this work

[4]Lead Contact

SUMMARY

Understanding and assessing endocrine response to stress is crucial to human performance analysis, stress-related disorder diagnosis, and mental health monitoring. Current approaches for stress monitoring are largely based on questionnaires, which could be very subjective. To avoid stress-inducing blood sampling and to realize continuous, non-invasive, and real-time stress analysis at the molecular levels, we investigate the dynamics of a stress hormone, cortisol, in human sweat using an integrated wireless sensing device. Highly sensitive, selective, and efficient cortisol sensing is enabled by a flexible sensor array that exploits the exceptional performance of laser-induced graphene for electrochemical sensing. Herein, we report the first cortisol diurnal cycle and the dynamic stress response profile constructed from human sweat. Our pilot study demonstrates a strong empirical correlation between serum and sweat cortisol, revealing exciting opportunities offered by sweat analysis toward non-invasive dynamic stress monitoring via wearable and portable sensing platforms.

Graphical Abstract

*Correspondence: weigao@caltech.edu.

AUTHOR CONTRIBUTIONS

W.G., R.M.T.R., and J.T. initiated the concept. W.G., R.M.T.R., J.T., and W.I. designed the experiments; R.M.T.R. and J.T. led the experiments and collected the overall data; Y.Y. performed electrode fabrication and characterization; J.M. performed the circuit design and test; C.X., C.Y., M.W., Y.S., and Y.Y. contributed to sensor characterization; W.G., R.M.T.R., and J.T. contributed the data analysis and co-wrote the paper. All authors provided the feedback on the manuscript.

DECLARATION OF INTEREST

The authors declare no competing financial interest.

DATA AVAILABILITY

The data that support the plots within this paper and other findings of this study are available from the corresponding author upon reasonable request.

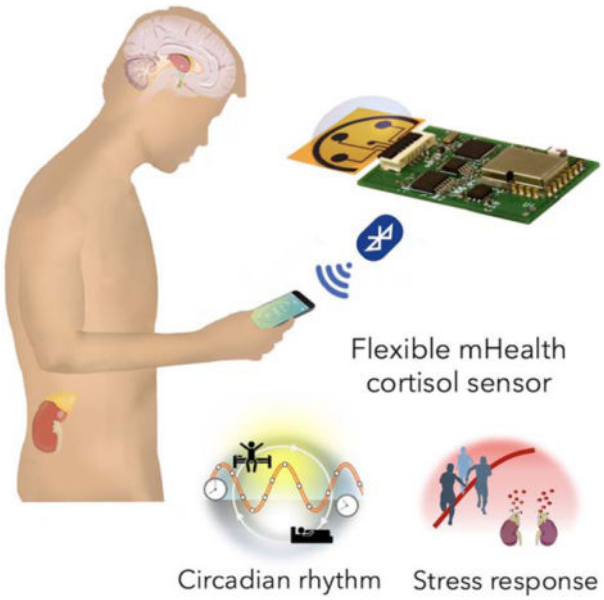

e-TOC

A fully integrated, flexible and miniaturized wireless mHealth sensing device based on laser-engraved graphene and immunosensing with proven utility for fast, reliable, sensitive and non-invasive monitoring of stress hormone cortisol is developed. Pilot human study results revealed a strong correlation between sweat and circulating hormone for the first time. Both cortisol diurnal cycle and dynamic stress response profiles were established from human sweat, reflecting the potential of such mHealth device in personalized healthcare and human performance evaluation.

Keywords

graphene; flexible sensors; mHealth; stress hormone; sweat; cortisol; stress response

INTRODUCTION

The exponential increase in the pace of life in the 21st century constantly demands intense and prolonged mental as well as physical efforts from individuals,[1] both of which are potential triggers of stress. Chronic stress has been associated with higher risks of anxiety, depression, suicide, weakening immune response as well as cardiovascular diseases (CVD).[2] The need for measurable stress indicators has never been more than apparent, be it in the contexts of posttraumatic stress disorder (PTSD) screening and depression evaluation, or a more general mental and somatic health monitoring setting. Although psychosocial and physiological stresses are induced by distinct stimuli, they share similar neuroendocrine and behavioral responses regulated by the hypothalamic-pituitary-adrenal (HPA) axis.[3] Activation of the HPA axis stimulates the secretion of glucocorticoids (e.g., cortisol), a group of hormones that mobilize energy in the body to cope with stress (Figure 1A).[4] While short-term alterations in the HPA axis are deemed as normal and adaptive responses of the body, chronic dysregulation of the HPA axis, an energetically costly state, is associated with

various pathological processes. As such, stress and individuals' stress-coping responses, are perceived as dynamic processes; absolute quantification of stress level provides much richer information and greater diagnostic value in the context of time and environment.[5]

Experience sampling methods (ESM) such as questionnaires and diary studies play a pivotal role in establishing the situational contexts of stressors in relevant longitudinal stress-response studies; however, their inherent idiosyncrasy imposed by subjective interpretations challenges the accuracy of "stress level" assessment.[6,7] Quantification of stress hormones in biological fluids provides measurable physiological indicators for mental distress. For example, the disturbances in circadian patterns of a key stress hormone, cortisol, are linked to PTSD and major depressive disorder (MDD) (Figure 1B).[8,9] In addition, the cortisol dynamics in stress response plays a crucial role in human performance (Figure 1C).[10] Other than the direct assessment of stress, stress hormones are also important in the understanding of pain and fear neural circuits,[11,12] both of which are subjective sensation or emotion that are hard to quantify. Blood test, albeit being the most well-studied hormone assessment method, is afflicted by its invasive nature and potential role as a stress stimulus. Saliva and sweat analyses, on the other hand, offer an attractive alternative for non-invasive stress hormones dynamics studies.

Recent advances in wearable and mobile health (mHealth) sensing systems have opened up a window of opportunities for hassle-free, real-time, personalized physiological data collection.[13–21] Substantial progress in the realm of wearable physical sensing platform has been made with systems capable of documenting physical and kinematic data such as temperature,[22] pulse rate[23] and ECG[24] in real time. Although human sweat contains rich health information and could allow non-invasive molecular monitoring, the majority of the wearable or portable systems available for sweat chemical biomarker dynamics studies are still limited to high concentration (usually at mM level) analytes like pH, sodium, chloride, and glucose.[25–30] To date, the reported sweat hormone sensors were generally characterized in either buffer or artificial sweat samples,[31,32] and the dynamics of the sweat stress hormones has not yet been well studied.

In this work, we investigate the dynamics of the sweat stress hormone using an integrated wireless mHealth device — graphene-based sweat stress sensing system (GS^4) (Figure 1A). As a proof-of-concept, cortisol is selected as the model stress hormone for dynamic profiling. Highly sensitive, selective, and efficient cortisol sensing in human sweat and saliva is achieved through a unique approach that combines the laser-induced graphene and competitive immunosensing. We report here, for the first time, the cortisol diurnal cycle and the dynamic stress response profile constructed from sweat using an integrated sensing device (Figure 1A). A strong correlation between sweat and serum cortisol levels are obtained from a small-scale pilot study. Such a wearable and point-of-care device-enabled non-invasive sweat analysis would add another dimension to stress monitoring since it offers minimal disturbance of daily routines and could provide instantaneous and continuous assessments on subjects' psychological state.

RESULTS AND DISCUSSION

Design of the graphene-based cortisol sensor

The key component of our GS[4] platform is a flexible five-electrode graphene sensor patch fabricated on a polyimide (PI) substrate via laser engraving as illustrated in Figure 1D–F. It boasts the advantage of rapid, scalable, and low-cost production (Figure 1E), and does not require elaborate lithography equipment or fabrication masks as compared with screen-printed electrodes. The flexible sensor patch consists of three graphene working electrodes (WEs), one Ag/AgCl reference electrode (RE), and one graphene counter electrode (CE) as it is depicted in Figure 1F. Detection of cortisol in human sweat is achieved through the combination of carboxylate-rich pyrrole-derivative grafting and subsequent modification on graphene surface and a competitive sensing strategy. The large surface area and fast electron mobility of graphene offers superior performance in electrochemical sensing (Figure 1G),[33] while competitive immunosensing strategies offer major advances in highly selective small hormone molecule detection.[34]

Electrochemical characterization and validation of the cortisol sensor

Figure 2A illustrates the process of sweat analysis and the sequential surface modification of graphene electrodes for cortisol determination, respectively. In the event of sweat analysis, sweat cortisol and horseradish peroxidase (HRP)-labeled cortisol compete for binding onto antibody-modified graphene electrode surface; enzymatic reduction of hydrogen peroxide mediated by hydroquinone (HQ) generates a cathodic current which is inversely proportional to the amount of cortisol in biofluids. The detailed surface modification procedure of graphene electrodes is schematized in Figure 2B and S1. Polymerization of pyrrole propionic acid (PPA) improves the strength and adhesion of polymeric films to transducer surfaces and facilitates subsequent surface modifications with carboxylate moieties for affinity-based sensor fabrication. In contrast to conventional graphene modification techniques such as acid reflux or monolayer formation of aryl hydrocarbon derivative, the electro-grafting of pyrrole-derivative is fast (~260 s), controlled, and scalable (by connecting electrodes in parallel). Upon electropolymerization of PPA, the graphene electrode is activated by 1-Ethyl-3-(3-dimethylaminopropyl)carbodiimide (EDC) and N-hydroxysulfosuccinimide (Sulfo-NHS) for covalent immobilization of anti-cortisol monoclonal antibody (mAb), followed by deactivation of unreacted sites with bovine serum albumin (BSA). This surface biomodification is universal to all bioaffinity receptors immobilization and could be adapted for other hormone antibodies. After brief incubation of the sensor with sweat containing the enzymatic tracer (HRP-labeled cortisol), amperometric response at −0.2 V (vs. Ag/AgCl) in the presence of detection substrate (HQ/H_2O_2) is recorded.

To confirm the successful sensor modification, material properties of the graphene surface are characterized by scanning electron microscopy (SEM), Raman spectroscopy and X-ray photoelectron spectroscopy (XPS) (Figure 2C–E). The decrease in I_D/I_G value in the Raman spectrum after surface modification implies the improvement of defect concentration after a thin uniform layer of pyrrole derivative is deposited (Figure 2D). The significantly increased N1s and S2p peaks in XPS (Figure 2E) indicate the successful activation of the surface and

the immobilization of the capture antibody (CAb) on the sensing electrode. Moreover, open circuit potential-electrochemical impedance spectroscopy (OCP-EIS) and differential pulse voltammetry (DPV) techniques are applied to electrochemically characterize the surface after each modification step involved in the affinity-based assay. Nyquist plots for the graphene electrode exhibit increasing resistance after each modification step as a consequence of impeded interfacial electron transfer between the redox probe in solution and the functionalized transducer surface (Figure 2F). The successful polymer deposition and the effective affinity bioreceptor immobilization on the modified-graphene surface are also confirmed by DPV (Figure S2). The effect of HRP-labeled cortisol concentration on amperometric responses is investigated. A dilution factor of 200 is chosen as it yields the largest ratio between currents for 0.0 ($I_{0.0}$) and 10.0 ng/mL ($I_{10.0}$) cortisol (Figure S3).

The performance of the as-prepared sensor is evaluated by measuring amperometric readout in phosphate buffered (PB) solutions containing varied cortisol concentrations (Figure 2G). Sensors prepared with laser-induced graphene electrodes (LGEs) demonstrate a much higher sensitivity with six- and nearly two-folds reduction in current density between 0.0 and 1.0 ng/mL (3.72 vs. 0.68 and 3.72 vs. 2.41 nA/mm^2) as compared with screen-printed carbon electrodes (SPCEs) and glassy carbon electrodes (GCE), respectively (Figure 2H). Amperometric signals (I) obtained with competitive strategies are best described by a sigmoidal curve using the four-parameter logistic (4-PL) model following the equation:[35]

$$I = i_1 + \frac{i_2 - i_1}{1 + 10^{(logIC_{50} - x) * p}}$$

where i_2 and i_1 indicate the maximum and minimum current values of the dose-response curve obtained; IC_{50} represents the level of cortisol at which amperometric signal decreases to 50% of the maximum current, x is the cortisol concentration in log scale, and p is the Hill slope at the inflection point of the sigmoid curve. Sigmoidal calibration plots of cathodic currents as a function of cortisol concentrations in buffer, sweat and saliva samples from a healthy subject are demonstrated in Figure 2I. No significant slope variations are observed between data obtained in human biospecimens and in buffered solutions. The limit of detection (LOD), calculated as the concentration of cortisol that produces 10% inhibition binding of HRP-labeled tracer to the immobilized affinity receptor (i.e., 10% signal reduction) is 0.08 ng/mL. The concentration range for 20%–80% inhibition binding of the enzymatic tracer is 0.43–50.2 ng/mL cortisol, covering the physiologically relevant range in sweat and saliva samples reported in previous studies.[36–38]

Considering that human sweat exhibits huge interpersonal variations in pH and salt content, the performance of the sensors under various pH levels and ionic strength conditions is evaluated (Figure S4A and S4B). The consistent sensor signals indicate the universality of the sigmoidal calibration curve constructed. In addition, the selectivity of our cortisol sensor is investigated by comparing the sensor responses in the presence of other non-target hormones. As illustrated in Figure S4C, no cross-reactivity is observed for β-estradiol, progesterone, and cortisone.

Target binding is the rate determining factor in bioaffinity sensors. To ensure rapid analysis and to allow sufficient time for binding, a crucial criterion at the point-of-care – the effect of competition time on sensor responses is investigated. Figure 2J shows the amperometric responses obtained for 0.0 and 5.0 ng/mL cortisol with different incubation times (30 seconds, 1, 5, 15, and 60 minutes). 15-minute recognition time is employed for real sample analysis presented in this work in order to ensure accurate quantitation of ultra-low levels of cortisol in biofluids with a high contrast-to-noise ratio. Here, the incubation time selected is based on the experimental observation of the optimum competition rate rather than the time for binding equilibrium, as the equilibrium time is long for a heterogeneous system. Nonetheless, significant competition (47%) is observed for 5.0 ng/mL cortisol with even 1-minute incubation, indicating that our sensor is capable of close to real-time analysis of sweat cortisol at ng/mL level (much faster compared to recent published sensing methodologies).[31, 38] One potential strategy to further shorten the incubation time is through enhanced mixing to promote the availability of unbound cortisol to antibodies on the graphene surface.

Endogenous circulating cortisol levels in human body fluids measured with the proposed methodology in human sweat samples (as well as saliva samples, collected from eight healthy participants) are validated with the gold standard enzyme-linked immunosorbent assay (ELISA). A high correlation between the results from the ELISA and the sensors (r = 0.973) is obtained (Figure 2K), endorsing the accuracy of rapid cortisol quantification with our device. In addition, the sensors retained good amperometric responses (> 90%) after storing at 4 °C for 7 days (Figure S5).

Systems integration and validation toward personalized sweat sampling and analysis

In the GS^4, a 3WE sensor array design with a Ag/AgCl RE and a graphene CE that provides simultaneous multichannel readings is employed. The multichannel design provides additional accuracy via signal averaging and could potentially be adapted as a hormone panel sensor for multiplexed detection of stress-related hormones. To minimize the variation of current readout due to the ohmic drop in a non-ideal electrochemical cell (Figure S6), the reference and counter electrodes are positioned in equidistance from each working electrode with a suitable geometric design shown in Figures 3A. A microfluidic module is integrated into the flexible graphene sensor patch to enable the on-body sweat sampling and in situ cortisol recognition (Figure 3A). This design minimizes the errors caused from the sweat evaporation and skin contamination from the traditional sweat collection, leading to nearly real-time stress hormone monitoring. Figure 3B illustrates block diagrams of functional units of the integrated electronic system that takes amperometric measurements from three channels concurrently, and wirelessly transmits the acquired data to a user device over Bluetooth Low Energy (BLE). The compact device, including a 3.7 V lithium-ion polymer battery mounted underneath a printed circuit board (PCB), is 20 mm × 35 mm × 7.3 mm in dimension. Fully functioning GS^4 drew 13.3 mA per second from a 150 mAh 3.7 V battery during an amperometric measurement, enabling 330-minute continuous amperometric measurements. The operation time can be significantly improved by incorporating the sleeping mode for the microcontroller and Bluetooth modules.

Representative 3-channel amperometric responses obtained with the GS^4 are demonstrated in Figure 3C. The calibration plot was constructed from the potential difference obtained with the GS^4 in the buffer solutions with five concentrations of cortisol in the pseudolinear region of the full sigmoidal plot (Figure 3C inset). It should be noted that stable wireless sensor readings can be achieved within 10-s measurement, indicating the rapid sensing capability of the GS^4. To validate that 3-channel averaging indeed provides more precise reading, we collected current readouts for 0.0, 1.0 and 5.0 ng/mL cortisol solutions from eight different sensors respectively. This is followed by enumerations of all 2-element and 3-element combinations of the datasets and random selection of eight combinations in Matlab to simulate 2-channel and 3-channel readings obtained with a sensor array. Error bars representing standard deviations of the simulated 2WE and 3WE readings demonstrate that the adoption of a 3WE system reduces inter-assay variation as shown in Figure 3D. Recovery study performed on a real human sweat sample spiked with 0.0, 1.0, 2.5 and 5.0 ng/mL cortisol using the GS^4 shows an average 94.2% recovery (Figure S7), suggesting a low systematic error.

The flexible, disposable microfluidic sensor patch shows excellent mechanical flexibility and can conformally laminate on the skin (Figure 3E). To demonstrate the influence of the mechanical deformation during the on-body recognition on the cortisol determination, responses of the flexible graphene sensor patch in 1.0, 5.0, and 10.0 ng/mL cortisol solutions incubated under different bending curvatures are recorded and illustrated in Figure 3F. No apparent variations in the sensor readouts are observed with or without deformation, indicating the great mechanical and electrochemical stability toward on-body use. Considering that the actual temperature of the sensor patch during sweat collection could be significantly higher than the room temperature (Figure S8), a temperature effect study was performed to evaluate the performance of the GS^4. The sensors present no significant variation in the signals obtained for 0.0, 1.0 and 5.0 ng/mL cortisol under varied temperatures (25, 31, and 37 °C) (Figure S9).

As compared to the current standard analytical methods for hormone analysis such as ELISA, the GS^4 has distinct capabilities in multiplexed monitoring, miniaturization, short assay time (down to 1 minute vs. 80 minutes), and smaller required sample volume (<10 μL vs. 100 μL), making it an ideal platform for subsequent investigations on dynamic sweat cortisol variations and potential applications in personalized health management.

Investigation of the circadian rhythm of sweat cortisol

Cortisol presents a distinct and robust diurnal pattern, which peaks shortly after awakening and declines throughout the day in plasma[40] and saliva.[41] Early report shows that sweat contains cortisol level comparable to those reported in saliva;[42] we postulate that, circulating cortisol molecules are transported to and stored in eccrine and apocrine glands, secreted into the sweat, and ultimately excreted through a sweat pore to the epidermal surface.[43] It is, therefore, reasonable to hypothesize that cortisol level in sweat might present similar circadian rhythm regulated by the internal clock and light/dark cycle (Figure 4A). Considering that circadian pattern of circulating cortisol is highly informative for a number of mental health conditions,[8,9] the fluctuations of the ultra-low levels of sweat cortisol are

investigated with the graphene platform through a pilot human study. Sweat was sampled with iontophoretic sweat stimulation as illustrated in Figure S10.

Figure 4B illustrates the reproducible patterns obtained from an exploratory study by monitoring the sweat cortisol variations of a healthy subject in a period of six days. High morning (AM) cortisol level and low afternoon (PM) level are observed each day; such rhythm resembles diurnal cycles of circulating cortisol in blood. In order to further characterize the correlation between sweat and circulating cortisol levels, sweat in the early AM and in the late PM from four healthy subjects are analyzed along with saliva and serum. A similar trend in AM/PM cortisol variations modulated by circadian rhythm are observed from all the samples (Figures 4C–F), with the ratios ranging from 1.35 to 2.00. Although several studies explored the correlation of cortisol found in various biofluids including blood, urine, and saliva,[44–46] the relationship between sweat and circulating cortisol levels, to the best of our knowledge, has barely been explored. A positive correlation between sweat cortisol and serum cortisol (Pearson's correlation coefficient $r = 0.87$) (Figure 4G) is obtained based on data collected from eight healthy subjects. Similarly, the correlation coefficient between sweat cortisol and salivary cortisol is determined to be 0.78 (Figure 4H). Although the number of real samples analyzed is limited in this exploratory study, empirical evidence suggests strong correlation exists between sweat cortisol and serum cortisol.

Dynamic cortisol response to stress stimuli

In addition to long-term profiling of the diurnal cycles, cortisol response to acute stressors contains abundant information for psychoneurological investigations,[47,48] and plays a critical role in human performance monitoring and management.[1] For instance, sensitization of the HPA axis to external stimuli is another critical factor that distinguishes PTSD from other psychiatric disorders.[8] Next, we set out to investigate if sweat analysis of cortisol presents meaningful changes to acute stress of the human subjects induced by different stressors in a short time frame. Aerobic exercises such as running and cycling are potent stimuli/stressor of cortisol secretion.[49] In this study, a 50-minute stationary cycling exercise at a constant workload is employed for sweat cortisol content analysis (Figure 5A). Sweat sampling and analysis are performed with the GS^4 sequentially at 10-minute intervals for the 50-minute constant-load exercise in a cycling ergometer from three physically untrained and one trained (athletic) subjects. In addition, serum cortisol levels before and immediately after the cycling exercise are analyzed to validate if sweat cortisol variation is in accordance with circulating cortisol levels. For all subjects under study, sweat cortisol increases progressively and reaches the highest level after 40 minutes of continuous biking. From this point, a slight decrease in cortisol level is detected near the end of the exercise in all participants and more significantly in subject 4 (athlete) (Figure 5B). Cortisol contents in pre- and post-exercise serum samples present good correlation to the change in cortisol from the beginning of the perspiration (10 minutes) to the end of the exercise (50 minutes) (Figure 5C). The dynamic sweat hormone profiles observed for untrained subjects are similar to reported trends of serum cortisol after high-intensity exercise,[50] indicating the activation of HPA by physical exercise. In contrast, the blunted cortisol response observed in the trained subject reflects exercise-induced adaptation. This is consistent with previous reports that trained individuals likely perceived the given workload as a smaller stressor and demonstrate

a lower degree of HPA activation in response to physical stressors[51] as well as psychosocial stimuli.[52]

Noting that circadian patterns in sweat cortisol level give rise to different baseline before stress stimulation, cortisol variations in sweat for physical exercises conducted in the morning and in the afternoon for the same subjects are studied. Sweat cortisol levels are analyzed from two subjects in the beginning of the perspiration and in the end of the cycling (Figure S11). Significantly increased sweat cortisol levels are observed at 50 minutes as compared to that at 10 minutes, in response to the physiological stressor. Cortisol level for the first time point is higher in the AM than in the PM for both subjects; higher relative percentage change of cortisol is observed in the PM exercise. This relation is in agreement with the diurnal sweat cortisol variation we observed in the circadian rhythm study, similar to a previous report that shows the circadian rhythm of serum and salivary cortisol could confound the magnitude of cortisol responses.[53] These results reveal the importance of baseline construction in offsetting circadian baseline in the context of short-term dynamic sweat cortisol stress response. Point-of-care and wearable devices-enabled sweat analysis could conveniently facilitate personalized baseline construction as discussed for the circadian rhythm study.

To study the response time frame of sweat cortisol to acute stressors, an exploratory cold pressor test (CPT) was performed on four subjects. Subjects were asked to immerse their non-dominant hand in ice water for 3 minutes (Figure 5D). CPT is a reliable acute physiological stressor that triggers immediate HPA axis activation and significant cortisol release.[54] Sweat was sampled at 8-minute interval with iontophoretic sweat stimulation as illustrated in Figure S10. Sweat dynamic cortisol profile was evaluated in each case and we observed that cortisol increased after completion of CPT, reaching the mean peak between 8 and 16 minutes after CPT (Figure 5E). Similar trends were also observed for serum (Figure 5F) and salivary cortisol (Figure S12); the former collected and tested before starting the experiment (denoted as baseline), 8 and 24 minutes after CPT. These observations are consistent with previously reported CPT studies for cortisol and other hormones release evaluation in serum[55] and saliva.[56] The sweat cortisol profiles presented small to negligible time lag as compared with serum cortisol trends in literature,[57–59] revealing the promptness of sweat cortisol as a quasi-real-time stress indicator. Furthermore, given the clinical applicability of CPT for pain tolerance evaluation,[60] sweat stress hormones sensors may serve as an attractive quantification approach in pain perception studies.

CONCLUSION

This work demonstrates the potential of sweat hormone analysis enabled by an integrated portable system – the GS[4]. Highly sensitive, selective, and efficient stress hormone sensing was achieved through a unique combination of the laser-induced graphene and immunosensing. The assay time could be as low as 1 minute. Using this graphene-based wireless sensing platform, we have demonstrated that relevant information crucial to stress response and adaptation analysis could be extracted from cortisol excreted in sweat. The low-cost and mass-produced graphene sensor arrays enabled us to conduct several meaningful stress-related physiological studies. To the best of our knowledge, the results we

present here represent the first demonstration of cortisol diurnal cycle and the dynamic stress response profile constructed from human sweat. On a longer timescale, characteristic cortisol circadian rhythms could be monitored; in a short time frame, acute external stimuli triggered stress response could be analyzed.

This study unveils the immense potential of sweat cortisol circadian variation monitoring. Sweat's accessibility to wearable continuous monitoring devices and its minimal invasiveness enables the construction of long-term and comprehensive cortisol diurnal patterns. To date, many clinical studies on psychological disorders-triggered cortisol circadian rhythms variation rely heavily on data collected at sparsely spaced plasma or saliva cortisol sampling timing[61,62] whereas those with narrow sampling intervals were achieved with intravenous catheters;[63] confirmation of cortisol circadian rhythms in sweat might revolutionize clinical research and mental health monitoring paradigm for both clinicians and patients in the near future.

The possibility of continuous dynamic stress response profiling with sweat sensors offers new opportunities for fundamental psychoneuroendocrinology studies and timely documentation of stress level for day-to-day mental health monitoring. Although only physical stress stimuli were investigated in the present study, given the fact that psychosocial stress stimuli trigger similar neuroendocrine and behavioral responses regulated by HPA axis,[3] similar information may be extracted from sweat cortisol in response to psychosocial stresses. The good correlation with circulating hormones, the diurnal cycle, and dynamic stress response profile demonstrated in this study using our integrated sensing approach will lead the next wave of technological advancement in personalized human performance and mental health management.

EXPERIMENTAL PROCEDURES

Materials and reagents

1-H pyrrole propionic acid (PPA, 97%), 1-ethyl-3-(3-dimethylamonipropyl)carbodiimide (EDC), N-hydroxysulfosuccinimide (Sulfo-NHS), bovine serum albumin (BSA), hydroquinone (HQ), 2-(N-morpholino)ethanesulfonic acid (MES), Tween® 20, hydrocortisone, cortisone, progesterone, β-estradiol, sodium thiosulfate, sodium bisulfite and potassium ferrocyanide (II) were purchased from Sigma Aldrich. Sodium dihydrogen phosphate, potassium hydrogen phosphate, potassium chloride, hydrogen peroxide (30% w/v) and sulfuric acid were purchased from Fischer Scientific. Potassium ferricyanide (III) and silver nitrate, iron (III) chloride and 0.1 M PBS (pH 7.4) were purchased from Across Organics and Alfa Aesar, respectively. Anti-cortisol murine monoclonal antibody and HRP-labeled cortisol were purchased from EastCoastBio. Cortisol competitive human ELISA kit (Catalog. No. EIAHCOR) was purchased from Thermo Fisher. Polyimide film (PI, 75 μm thick) was purchased from DuPont.

Fabrication of three channel array electrode

For three channel graphene sensor fabrication, a PI film was attached onto a supporting substrate in a 50 W CO_2 laser cutter (Universal Laser System). Selected laser-cutting

parameters were: Power 5.0%, Speed 6%, Points Per Inch (PPI) 1000, in raster mode and at focused height. Ag/AgCl reference electrodes (RE) were fabricated by electrodeposition in 20 μL of a mixture solution containing silver nitrate, sodium thiosulfate, and sodium bisulfite (final concentrations 250 mM, 750 mM and 500 mM, respectively) for 100 seconds at −0.2 mA, followed by drop casting 10 μL-aliquot of $FeCl_3$ for 1 minute.

Modification of sensing platform and electrochemical detection

PPA electropolymerization was conducted by CV from 0.0 to 0.85 V (vs. Ag/AgCl) for 20 cycles at a scan rate of 0.1 V/s in a fresh solution containing 5.0 mM carboxyl-functionalized pyrrole monomer and 0.5 M KCl. After rinsing with deionized (DI) water and drying under air flow, electrodes were incubated with 10 μL of a mixture solution containing 0.4 M EDC and 0.1 M Sulfo-NHS in 0.025 M MES, pH 5.0, for 35 minutes at room temperature under humid ambient conditions. Covalent attachment of specific antibody onto activated surface was carried out by drop casting 10 μL of anti-cortisol antibody solution (100 μg/mL in MES buffer, pH 5.0) and incubated at room temperature for 90 minutes, followed by a 1 hour blocking step with 1.0% BSA prepared in 0.01 M phosphate buffered saline with Tween® 20 (PBST) of pH 7.4. After one washing step with same buffered solution, 10 μL-aliquots of cortisol standards (or the biofluid to be analyzed properly diluted) and HRP-cortisol (1/200 dilution) prepared in PBST, pH 7.4, were drop casted onto the working electrode, allowing competition between labeled and circulating free cortisol contained in the sample for the available free sites of the immobilized affinity receptor to take place for 15 minutes. Amperometric readings were registered at −0.2 V (vs. Ag/AgCl) in 50 mM sodium phosphate buffer of pH 6.0 containing 2.0 mM HQ. The readout signal was obtained after a 30 μL-aliquot of 10 mM H_2O_2 was injected to the system.

Characterization of the biosensing platform

The morphology and material properties of the graphene sensing electrodes before and after surface modification were characterized by TEM, SEM, Raman and XPS. The SEM images of graphene electrodes were obtained by focused ion beam SEM (FIB–SEM, FEI Nova 600 NanoLab). TEM images were obtained by transmission electron microscope (TecnaiTF-20). The surface properties of the laser-induced graphene were characterized by X-ray photoelectron spectroscopy (Escalab 250xi, Thermo Scientific). Raman spectrum of the graphene was recorded using a 532.8 nm laser with an inVia Reflex (Renishaw, UK).

Amperometry, open circuit potential-electrochemical impedance spectroscopy (OCP-EIS), cyclic voltammetry (CV), and differential pulse voltammetry (DPV) were carried out on a CHI820 electrochemical station by means of an electrochemical setup comprising laser-induced graphene electrodes (LGEs) as the working electrodes (WEs), a platinum wire as the counter electrode (CE), and a commercial Ag/AgCl electrode as the reference electrode (RE).

In order to characterize surface modification after each step electrochemically, DPV and OCP-EIS readings were carried out in 0.01 M PBS, pH 7.4, containing 2.0 mM of $K_4Fe(CN)_6/K_3Fe(CN)_6$ (1:1) at detailed conditions: potential range, −0.3 and 0.6 V; pulse width, 0.2 s; incremental potential, 4 mV; amplitude, 50 mV; frequency range, 0.1–10^6 Hz;

amplitude, 5 mV. Performances of LGEs, glassy carbon electrodes (GCEs) and commercial screen-printed carbon electrodes (SPCEs) were compared through current densities (nA/mm^2) obtained after developing the proposed competitive-based assay on both carbon surfaces for target cortisol determination at 1.0 and 5.0 ng/mL levels under optimized conditions. Dilution of HRP labeled cortisol was optimized by comparing amperometric responses obtained for 1/100, 1/200 and 1/300 diluted enzymatic tracer for 0.0 and 10.0 ng/mL cortisol standards. Performance of our device was evaluated for different pHs and salt contents ranging from 7.1 to 4.1 and from 0.1 M PBST to 0.001 M PBST, respectively. Selectivity test was conducted in the presence of mixture solutions of 1/200 HRP-cortisol enzymatic tracer containing 5.0 ng/mL cortisone, progesterone or β-estradiol, in the absence or in the presence of target hormone at the same concentration level. Stability study was conducted for target cortisol determination at 5.0 ng/mL levels under optimized conditions. The electrodes for stability study were modified on the same day and stored at 4 °C for 0 to 35 days before carrying out the competitive assay.

System level development and evaluation

The electronic system for the integrated three channel electrochemical analyzer was designed to be compact and efficient. A two-layer printed circuit board (PCB) (20 mm × 35 mm × 0.6 mm) had all the components on the top layer such that a 150 mAh 3.7 V lithium-ion polymer battery (19.75 mm × 26 mm × 3.8 mm) could sit comfortably underneath the PCB. The entire device is 20 mm × 35 mm × 7.3 mm, comparable to a USB thumb drive.

The small size, low power consumption, and rich analog peripherals of the STM32L432 ultra-low-power Arm Cortex-M4 32-bit microcontroller (MCU) enabled the compact size of the overall electronic system. The MCU had a built in 12-bit analog-to-digital converter (ADC) and two built-in 12-bit digital-to-analog converters (DAC). When a user initiates an electrochemical measurement over Bluetooth, the built-in DACs generate a reference voltage (V_{ref}) and a working voltage (V_w) that set the potentials at the reference electrode and working electrodes through a potentiostat interface circuit. For the 3-channel amperometric measurements required for cortisol analysis, the reference voltage was stabilized further by a low pass filter (LPF), and the three working electrodes were biased at −0.2 V relative to the reference electrode. The resultant currents flowing through each electrode were amplified and converted to voltage by transimpedance amplifiers (TIA). Three channels of the MCU's ADC were utilized to acquire concurrent amperometric measurements, and the data was transmitted to a user device over Bluetooth for further analysis.

To prepare the microfluidic module, a double-sided medical adhesive was attached to a substrate and cut through to make the channels and reservoir using a 50 W CO_2 laser cutter (Universal Laser System). Influence of mechanical deformation was investigated through incubating the sensor patch in the cortisol solutions for 15 minutes under mechanical deformation (with radii of bending curvature 2.3 and 3.8 cm).

Subjects and procedures

The performance of the GS^4 was evaluated in human sweat, saliva and sweat samples from the human subjects in compliance with the protocols that were approved by the institutional

review board (IRB) (No. 19–0895 and No. 19–0892) at California Institute of Technology (Caltech). The participating subjects (twelve healthy subjects, age range 18–65) were recruited from Caltech campus and the neighboring communities through advertisement by posted notices, word of mouth, and email distribution. All subjects gave written, informed consent before participation in the study.

Circadian rhythm study

Four healthy subjects who reported regular sleep-wake rhythm and no sleep disturbances participated in this study. Subjects were informed to refrain from food intake at least 30 minutes before reporting to the laboratory. On experimental day, subjects reported to the laboratory at 8:00 AM and at 7:00 PM on the same day for sweat, saliva and capillary blood collection. Sweat stimulation was performed with a Model 3700 Macroduct® by placing two electrodes on the pre-cleaned forearm region of the subject. After their connection to the source, a 1.5 mA current was applied for 5 minutes and secreted sweat was sampled for a period of 40 minutes and then analyzed. During the sweat sampling and test, fresh capillary blood and saliva were collected from subject immediately after sweat stimulation following the protocol described in the sample processing section.

Physiological stress response - stationary biking study

Three untrained participants and one trained participant were involved in this study. The trained subject (an athlete from Caltech sport teams) exercised regularly for at least 9 hours per week while the untrained subjects had an average of 1 hour of exercise per week. Constant workload physical activity trials were performed in the morning (ranging from 8:00 to 10:00, denoted as AM) or afternoon (from 5:00 to 7:00, denoted as PM) in an ergometer stationary bike (Kettler Axos Cycle M-LA). Subjects were informed to refrain from food intake at least 30 minutes before the exercise. Subjects were asked to bike for 50 minutes at a constant speed of 60 revolutions per minute (rpm) and sweat samples were collected every 10 minutes from the forehead. Before starting the aerobic trial, and after sweat sampling and analysis at each time interval, participants' foreheads were cleaned with alcohol swabs and gauze. Blood collection were performed before the stationary bike exercise and immediately after the exercise following the procedures described in sample processing protocol section.

Physiological stress response - cold pressor test

Four participants were exposed to standard CPT in the afternoon (between 5:00 to 7:00 PM) in order to control for the diurnal cortisol cycle. The experimental procedure was initiated by collecting sweat through iontophoresis for a period of 8 minutes. At the same time, saliva and capillary blood sample from each participant were collected with the purpose of determining baseline values. Subsequently, recruited volunteers immersed their non-dominant hand up to the wrist in a plastic tank containing cold-water (2 °C) for 3 minutes (CPT) and after the immersion time they were instructed to remove the hand from the ice-water. Sweat, saliva and capillary blood were collected following the detailed protocols at different resting periods after CPT test (8, 16, and 24 minutes).

Saliva and blood sample processing protocol

After rinsing mouth with water, volunteers deposited saliva in 1.5 mL Eppendorf tubes which were subsequently centrifuged (10000 rpm, 10 minutes) and analyzed. Fresh capillary blood samples were collected at same periods of time as saliva using a finger-prick approach. After cleaning the fingertip with alcohol wipe and allowing it to air dry, the skin was punctured with CareTouch lancing device. Samples were collected with 1.5 mL Eppendorf tubes after wiping off the first drop of blood with gauze. Once standardized clotting procedure finished, serum was separated by centrifuging at 3575 rpm for 15 minutes, and instantly stored at −20 °C.

Enzyme-linked immunosorbent assay for human sample analysis validation

ELISA tests for cortisol were performed in an accuSkan™ FC Filter-Based Microplate Photometer at a detection wavelength of 450 nm, according to the manufacturer's instructions. Briefly, standards (or properly diluted samples), HRP-cortisol conjugate and cortisol antibody were added to IgG coated microtiter plate wells and incubated during 1 hour at room temperature. After four washing steps with wash buffer, 100 μL of 3,3′,5,5′-Tetramethylbenzidine (TMB) substrate was incubated for 30 minutes and absorbance values were measured immediately after addition of 50 μL of 1M H_2SO_4 in each well.

Thermal imaging of device and skin temperature

Thermal images of the sensor patch on human skin were taken by a long wave infrared thermal camera (FLIR A655sc).

Supplementary Material

Refer to Web version on PubMed Central for supplementary material.

ACKNOWLEDGEMENTS

This project was supported by the Rothenberg Innovation Initiative (RI^2) program, the Carver Mead New Adventures Fund, Caltech-City of Hope Biomedical Research Initiative, and National Institute of Health (#5R21NR018271) (all to W.G.). J.T. was supported by the National Science Scholarship (NSS) from the Agency of Science Technology and Research (A*STAR) Singapore. We gratefully acknowledge critical support and infrastructure provided for this work by the Kavli Nanoscience Institute and Jim Hall Design and Prototyping Lab at Caltech, and we gratefully thank Dr. Matthew Hunt and Bruce Dominguez for their help. We also thank Dr. Chiara Daraio and Vincenzo Costanza for the technical support and helpful assistance with IR imaging.

REFERENCES

1. Mariotti A (2015). The effects of chronic stress on health: new insights into the molecular mechanisms of brain–body communication. Futur. Sci. OA 1, FSO23.
2. Cohen S, Janicki-Deverts D, and Miller GE (2007). Psychological Stress and Disease. J. Am. Med. Assoc 298, 1685–1687.
3. Kogler L, Müller VI, Chang A, Eickhoff SB, Fox PT, Gur RC, and Derntl B (2015). Psychosocial versus physiological stress — Meta-analyses on deactivations and activations of the neural correlates of stress reactions. NeuroImage 119, 235–251. [PubMed: 26123376]
4. Herman JP, McKlveen JM, Ghosal S, Kopp B, Wulsin A, Makinson R, Scheimann J, and Myers B (2016). Regulation of the hypothalamic-pituitary-adrenocortical stress response. Compr. Physiol 6, 603–621. [PubMed: 27065163]

5. Nicolson NA and Csikszentmihalyi M, “Stress, coping and cortisol dynamics in daily life,” in The Experience of Psychopathology: Investigating Mental Disorders in their Natural Settings (ed. de Vries MW), 219–232 (Cambridge University Press, 1992)
6. Sladek MR, Doane LD, and Stroud CB (2016). Individual and day-to-day differences in active coping predict diurnal cortisol patterns among early adolescent girls. J. Youth Adolesc 46, 121–135. [PubMed: 27783306]
7. Verhagen SJW, Hasmi L, Drukker M, Os JV, and Delespaul PAEG (2016). Use of the experience sampling method in the context of clinical trials. Evid.-Based Ment. Health. 19, 86–89.
8. Yehuda R (1997). Sensitization of the hypothalamic-pituitary-adrenal axis in posttraumatic stress disorder. Ann. N. Y. Acad. Sci 821, 57–75. [PubMed: 9238194]
9. Herbert J (2012). Cortisol and depression: three questions for psychiatry. Psychol. Med 43, 449–469. [PubMed: 22564216]
10. Bos RVD, Harteveld M, and Stoop H (2009). Stress and decision-making in humans: Performance is related to cortisol reactivity, albeit differently in men and women. Psychoneuroendocrinology 34, 1449–1458 [PubMed: 19497677]
11. Rodrigues SM, Ledoux JE, and Sapolsky RM (2009). The influence of stress hormones on fear circuitry. Annu. Rev. Neurosci 32, 289–313. [PubMed: 19400714]
12. Uum SHMV, Sauvé B, Fraser LA, Morley-Forster P, Paul TL, and Koren G (2008). Elevated content of cortisol in hair of patients with severe chronic pain: A novel biomarker for stress. Stress 11, 483–488. [PubMed: 18609301]
13. Kim J, Campbell AS, Ávila BE-FD, and Wang J (2019). Wearable biosensors for healthcare monitoring. Nat. Biotechnol 37, 389–406. [PubMed: 30804534]
14. Nakata S, Shiomi M, Fujita Y, Arie T, Akita S, and Takei K (2018). A wearable pH sensor with high sensitivity based on a flexible charge-coupled device. Nat. Electron 1, 596–603.
15. Lee H, Choi TK, Lee YB, Cho HR, Ghaffari R, Wang L, Choi HJ, Chung TD, Lu N, Hyeon T, et al. (2016). A graphene-based electrochemical device with thermoresponsive microneedles for diabetes monitoring and therapy. Nat. Nanotechnol 11, 566–572. [PubMed: 26999482]
16. Lee H, Song C, Hong YS, Kim MS, Cho HR, Kang T, Shin K, Choi SH, Hyeon T, and Kim D-H (2017). Wearable/disposable sweat-based glucose monitoring device with multistage transdermal drug delivery module. Sci. Adv 3, e1601314. [PubMed: 28345030]
17. Han S, Kim J, Won SM, Ma Y, Kang D, Xie Z, Lee K-T, Chung HU, Banks A, Min S, et al. (2018). Battery-free, wireless sensors for full-body pressure and temperature mapping. Sci. Transl. Med 10, eaan4950. [PubMed: 29618561]
18. Yang Y and Gao W (2019). Wearable and flexible electronics for continuous molecular monitoring. Chem. Soc. Rev 48, 1465–1491. [PubMed: 29611861]
19. Bariya M, Nyein HYY, and Javey A (2018). Wearable sweat sensors. Nat. Electron 1, 160–171.
20. Reeder JT, Choi J, Xue Y, Gutruf P, Hanson J, Liu M, Ray T, Bandodkar AJ, Avila R, Xia W, et al. (2019). Waterproof, electronics-enabled, epidermal microfluidic devices for sweat collection, biomarker analysis, and thermography in aquatic settings. Sci. Adv 5, eaau6356. [PubMed: 30746456]
21. Bandodkar AJ, Gutruf P, Choi J, Lee K, Sekine Y, Reeder JT, Jeang WJ, Aranyosi AJ, Lee SP, Model JB, et al. (2019). Battery-free, skin-interfaced microfluidic/electronic systems for simultaneous electrochemical, colorimetric, and volumetric analysis of sweat. Sci. Adv 5, eaav3294. [PubMed: 30746477]
22. Zhu C, Chortos A, Wang Y, Pfattner R, Lei T, Hinckley AC, Pochorovski I, Yan X, To JW-F, Oh JY, et al. (2018). Stretchable temperature-sensing circuits with strain suppression based on carbon nanotube transistors. Nat. Electron 1, 183–190.
23. Boutry CM, Beker L, Kaizawa Y, Vassos C, Tran H, Hinckley AC, Pfattner R, Niu S, Li J, Claverie J et al. (2019). Biodegradable and flexible arterial-pulse sensor for the wireless monitoring of blood flow. Nat. Biomed. Eng 3, 47–57. [PubMed: 30932072]
24. Son D, Kang J, Vardoulis O, Kim Y, Matsuhisa N, Oh JY, Mun J, Katsumata T, Liu Y, McGuire AF, et al. (2018). An integrated self-healable electronic skin system fabricated via dynamic reconstruction of a nanostructured conducting network. Nat. Nanotechnol 13, 1057–1065. [PubMed: 30127474]

25. Gao W Emaminnejad S, Nyein HYY, Challa S, Chen K, Peck A, Fahad HM, Ota H, Shiraki H, Kiriya D, et al. (2016). Fully integrated wearable sensor arrays for multiplexed in situ perspiration analysis. Nature 529, 509–514. [PubMed: 26819044]
26. Choi J, Bandodkar AJ, Reeder JT, Ray TR, Turnquist A, Kim SB, Nyberg N, Hourlier-Fargette A, Model JB, Aranyosi AJ, et al. (2019). Soft, Skin-integrated multifunctional microfluidic systems for accurate colorimetric analysis of sweat biomarkers and temperature. ACS Sens. 4, 379–388. [PubMed: 30707572]
27. Heikenfeld J Jajack A, Feldman B, Granger SW, Gaitonde S, Begtrup G, and Katchman BA (2019). Accessing analytes in biofluids for peripheral biochemical monitoring. Nat. Biotechnol 37, 407–419. [PubMed: 30804536]
28. Kim J, Jeerapan I, Imani S, Cho TN, Bandodkar AJ, Cinti S, Mercier PP, and Wang J (2016). Noninvasive alcohol monitoring using a wearable tattoo-based iontophoretic-biosensing system. ACS Sens. 1, 1011–1019.
29. Tai L-C, Gao W, Chao M, Bariya M, Ngo QP, Shahpar Z, Nyein HYY Park H, Sun J, Jung J et al. (2018). Methylxanthine drug monitoring with wearable sweat sensors. Adv. Mater 30, 1707442.
30. Emaminejad S, Gao W, Wu E, Davies ZA, Nyein HYY, Challa S, Ryan SP, Fahad HM, Chen K, Shahpar Z et al. (2017). Autonomous sweat extraction and analysis applied to cystic fibrosis and glucose monitoring using a fully integrated wearable platform. Proc. Natl. Acad. Sci. U.S.A 114, 4625–4630. [PubMed: 28416667]
31. Kinnamon D, Ghanta R, Lin K-C, Muthukumar S, and Prasad S (2017). Portable biosensor for monitoring cortisol in low-volume perspired human sweat. Sci. Rep 7, 13312. [PubMed: 29042582]
32. Parlak O, Keene ST, Marais A, Curto VF, and Salleo A (2018). Molecularly selective nanoporous membrane-based wearable organic electrochemical device for noninvasive cortisol sensing. Sci. Adv 4, eaar2904 [PubMed: 30035216]
33. Shao Y, Wang J, Wu H, Liu J, Aksay IA, and Lin Y (2010). Graphene based electrochemical sensors and biosensors: a review. Electroanalysis 22, 1027–1036.
34. Wang X, Cohen L, Wang J, and Walt DR (2018). Competitive immunoassays for the detection of small molecules using single molecule arrays. J. Am. Chem. Soc 140, 18132–18139. [PubMed: 30495929]
35. Findlay JWA and Dillard RF (2007). Appropriate calibration curve fitting in ligand binding assays. AAPS J. 9, E260–E267. [PubMed: 17907767]
36. Jia M, Chew WM, Feinstein Y, Skeath P, and Sternberg EM (2016). Quantification of cortisol in human eccrine sweat by liquid chromatography – tandem mass spectrometry. Analyst 141, 2053–2060. [PubMed: 26858998]
37. Miller R, Plessow F, Rauh M, Gröschl M, and Kirschbaum C (2013). Comparison of salivary cortisol as measured by different immunoassays and tandem mass spectrometry. Psychoneuroendocrinology 38, 50–57. [PubMed: 22641005]
38. Khan MS, Misra SK, Wang Z, Daza E, Schwartz-Duval AS, Kus JM, Pan D, and Pan D (2017). Paper-based analytical biosensor chip designed from Graphene-nanoplatelet-amphiphilic-diblock-co-polymer composite for cortisol detection in human saliva. Anal. Chem 89, 2107–2115. [PubMed: 28050904]
39. Laudat MH, Cerdas S, Fournier C, Guiban D, Guilhaume B, and Luton JP (1988). Salivary cortisol measurement: a practical approach to assess pituitary-adrenal function. J. Clin. Endocrinol. Metab 66, 343–348. [PubMed: 2828410]
40. Oster H, Challet E, Ott V, Arvat E, de Kloet ER, Dijk DJ, Lightman S, Vgontzas A, and Van Cauter E (2016). The functional and clinical significance of the 24-h rhythm of circulating glucocorticoids. Endocr. Rev 38, 3–45.
41. Ivars K, Nelson N, Theodorsson A, Theodorsson E, Ström JO, and Mörelius E (2015). Development of salivary cortisol circadian rhythm and reference intervals in full-term infants. PLOS One 10, e0129502. [PubMed: 26086734]
42. Russell E, Koren G, Rieder M, and Uum SHMV (2013). The detection of cortisol in human sweat. Ther. Drug Monit 36, 30–34.

43. Katchman BA, Zhu M, Christen JB, and Anderson KS (2018). Eccrine sweat as a biofluid for profiling immune biomarkers. Proteom. Clin. Appl 12, 1800010.
44. Burke PM, Reichler RJ, Smith E, Dugaw K, McCauley E, and Mitchell J (1985). Correlation between serum and salivary cortisol levels in depressed and nondepressed children and adolescents. Am. J. Psychiatry 142, 1065–1067. [PubMed: 4025623]
45. Vanbruggen MD, Hackney AC, Mcmurray RG, and Ondrak KS (2011). The relationship between serum and salivary cortisol levels in response to different intensities of exercise. Int. J. Sports Physiol. Perform 6, 396–407. [PubMed: 21911864]
46. Jung C, Greco S, Nguyen HH, Ho JT, Lewis JG, Torpy DJ, and Inder WJ (2014). Plasma, salivary and urinary cortisol levels following physiological and stress doses of hydrocortisone in normal volunteers. BMC Endocr. Disord 14, 91. [PubMed: 25425285]
47. Dickerson SS and Kemeny ME (2004). Acute stressors and cortisol responses: a theoretical integration and synthesis of laboratory research. Psychol. Bull 130, 355–391. [PubMed: 15122924]
48. Kudielka BM and Wüst S (2010). Human models in acute and chronic stress: Assessing determinants of individual hypothalamus–pituitary–adrenal axis activity and reactivity. Stress 13, 1–14. [PubMed: 20105052]
49. Kanaley JA (2001). Cortisol and growth hormone responses to exercise at different times of day. J. Clin. Endocrinol. Metab 86, 2881–2889. [PubMed: 11397904]
50. Weise M, Drinkard B, Mehlinger SL, Holzer SM, Eisenhofer G, Charmandari E, Chrousos GP, and Merke DP (2004). Stress dose of hydrocortisone is not beneficial in patients with classic congenital adrenal hyperplasia undergoing short-term, high-intensity exercise. J. Clin. Endocrinol. Metab 89, 3679–3684. [PubMed: 15292287]
51. Luger A, Deuster PA, Kyle SB, Gallucci WT, Montgomery LC, Gold PW, Loriaux DL, and Chrousos GP (1987). Acute hypothalamic–pituitary–adrenal responses to the stress of treadmill exercise. N. Engl. J. Med 316, 1309–1315. [PubMed: 3033504]
52. Rimmele U, Zellweger BC, Marti B, Seiler R, Mohiyeddini C, Ehlert U, and Heinrichs M (2007). Trained men show lower cortisol, heart rate and psychological responses to psychosocial stress compared with untrained men. Psychoneuroendocrinology 32, 627–635. [PubMed: 17560731]
53. Thuma JR, Gilders R, Verdun M, and Loucks AB (1995). Circadian rhythm of cortisol confounds cortisol responses to exercise: implications for future research. J. Appl. Physiol 78, 1657–1664. [PubMed: 7649899]
54. Schwabe L, Haddad L, and Schachinger H (2008). HPA axis activation by a socially evaluated cold-pressor test. Psychoneuroendocrinology 33, 890–895. [PubMed: 18403130]
55. Zimmer C, Basler H-D, Vedder H, and Lautenbacher S (2003). Sex differences in cortisol response to noxious stress. Clin. J. Pain 19, 233–239. [PubMed: 12840617]
56. Goodin BR, Smith MT, Quinn NB, King CD, and Mcguire L (2012). Poor sleep quality and exaggerated salivary cortisol reactivity to the cold pressor task predict greater acute pain severity in a non-clinical sample. Biol. Psychol 91, 36–41. [PubMed: 22445783]
57. Mcrae AL, Saladin ME, Brady KT, Upadhyaya H, Back SE, and Timmerman MA (2006). Stress reactivity: biological and subjective responses to the cold pressor and Trier Social stressors. Hum. Psychopharmacol 21, 377–385. [PubMed: 16915579]
58. Bullinger M, Naber D, Pickar D, Cohen RM, Kalin NH, Pert A, and Bunney WE Jr. (1984). Endocrine effects of the cold pressor test: Relationships to subjective pain appraisal and coping. Psychiatry Res. 12, 227–233. [PubMed: 6093173]
59. Geliebter A, Gibson CD, Hernandez DB, Atalayer D, Kwon A, Lee MI, Mehta N, Phair D, and Gluck ME (2012). Plasma cortisol levels in response to a cold pressor test did not predict appetite or ad libitum test meal intake in obese women. Appetite 59, 956–959. [PubMed: 22983369]
60. Mitchell LA, Macdonald RA, and Brodie EE (2004). Temperature and the cold pressor test. J. Pain 5, 233–237. [PubMed: 15162346]
61. Machale S Cavanagh JT, Bennie J, Carroll S, Goodwin GM, and Lawrie SM (1998). Diurnal variation of adrenocortical activity in chronic fatigue syndrome. Neuropsychobiology 38, 213–217. [PubMed: 9813459]

62. Strickland P, Morriss R, Wearden A, and Deakin B (1998). A comparison of salivary cortisol in chronic fatigue syndrome, community depression and healthy controls. J. Affect. Disord 47, 191–194. [PubMed: 9476760]

63. Vythilingam M, Gill JM, Luckenbaugh DA, Gold PW, Collin C, Bonne O, Plumb K, Polignano E, West K, and Charney D (2010). Low early morning plasma cortisol in posttraumatic stress disorder is associated with co-morbid depression but not with enhanced glucocorticoid feedback inhibition. Psychoneuroendocrinology 35, 442–450. [PubMed: 19766403]

Progress and Potential

Prompt and accurate detection of stress is essential to the monitoring and management of mental health and human performance. Considering that current methods such as questionnaires are very subjective, we propose a highly sensitive, selective, miniaturized mHealth device based on laser-enabled flexible graphene sensor to non-invasively monitor the level of stress hormones (e.g., cortisol). We report a strong correlation between sweat and circulating cortisol and demonstrate the prompt determination of sweat cortisol variation in response to acute stress stimuli. Moreover, we demonstrate, for the first time, the diurnal cycle and stress response profile of sweat cortisol, revealing the potential of dynamic stress monitoring enabled by this mHealth sensing system. We believe that this platform could contribute to fast, reliable and decentralized healthcare vigilance at the metabolic level, thus providing an accurate snapshot of our physical, mental and behavioral changes.

Highlights

- A fully integrated, flexible, and wireless device for sweat cortisol monitoring
- Mass-producible graphene sensor array for sensitive and reliable measurements
- A strong correlation between serum and sweat cortisol is obtained
- The diurnal cycle and stress response profile of sweat cortisol are reported

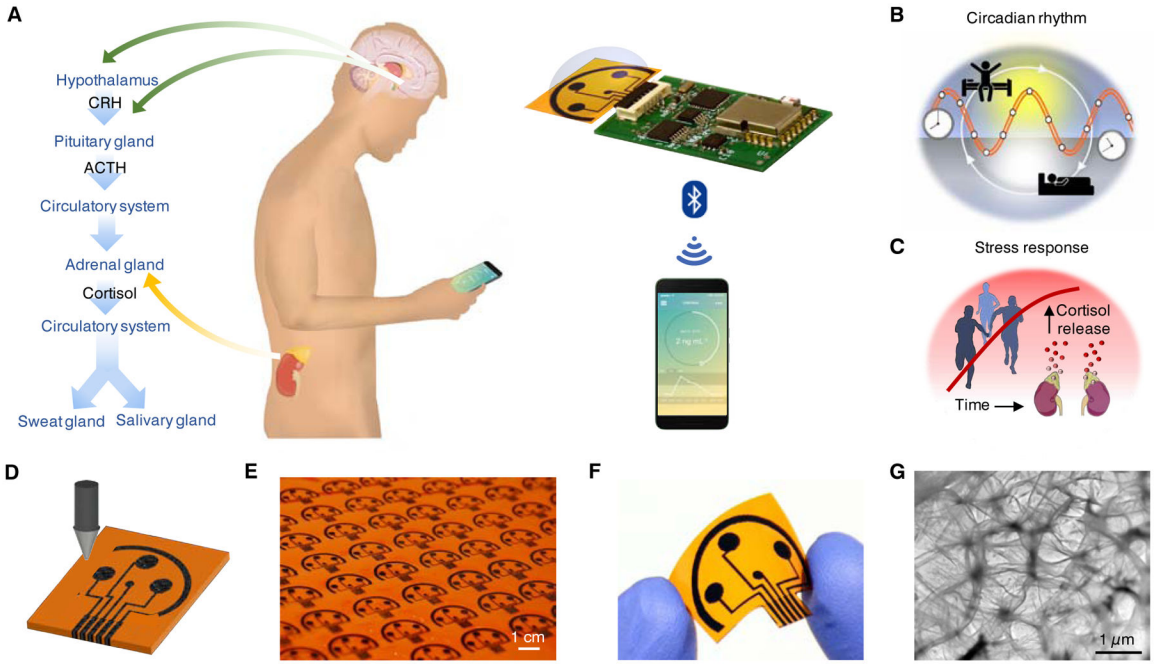

Figure 1. An integrated wireless graphene-based sweat stress sensing system (GS^4) for dynamic and non-invasive stress hormone analysis.

(A) Schematic illustration of the origin of cortisol in sweat and saliva and the use of the GS^4 to track the circulating cortisol level. CRH, corticotrophin-releasing hormone; ACTH, adrenocorticotropic hormone.

(B and C) Conceptual illustration of cortisol dynamics regulated by circadian rhythm (B) and triggered by physiological and psychological stress (C).

(D) Illustration of the laser engraving process of a graphene platform.

(E) Graphene sensor arrays mass-produced on a polyimide (PI) substrate.

(F) Image of a disposable flexible graphene sensor array.

(G) Transmission electron microscopy (TEM) image of the graphene electrode surface.

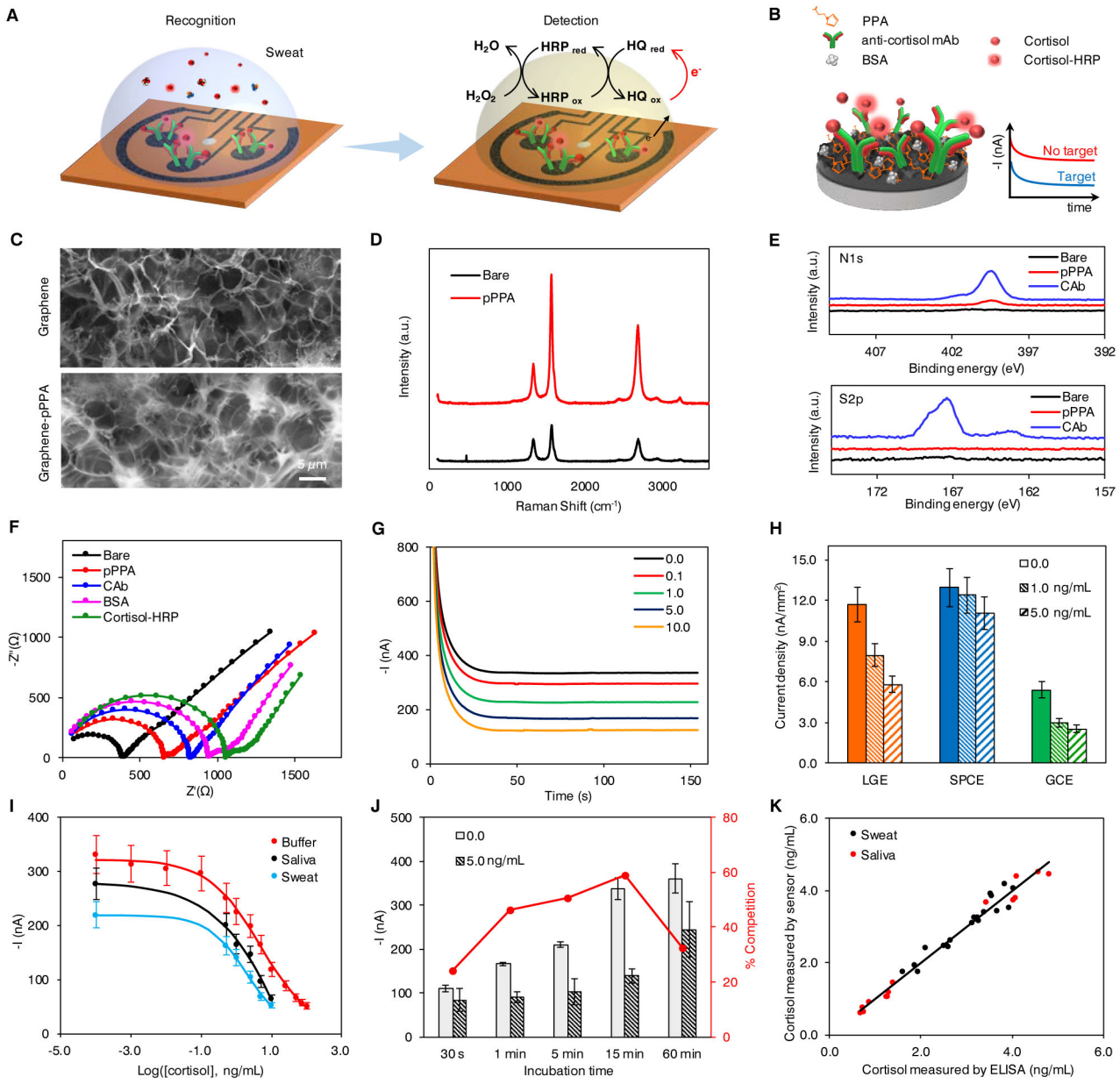

Figure 2. Characterization and validation of the electrochemical sensor for non-invasive cortisol analyses.

(A and B) Schematic of the electrochemical detection of cortisol in human sweat (A) and representation of the affinity-based electrochemical cortisol sensor construction and sensing strategy (B). HRP, horseradish peroxidase; HQ, hydroquinone; PPA, pyrrole propionic acid; BSA, bovine serum albumin; mAb, monoclonal antibody.

(C) Scanning electron microscopy (SEM) images of the graphene electrode surface before and after PPA polymerization.

(D and E) Raman spectra (D) and X-ray photoelectron spectra (E) of bare graphene electrode, and graphene electrodes modified with PPA (pPPA) and capture antibody (CAb).

(F) Nyquist plots of a graphene electrode in a 0.01 M PBS solution containing 2.0 mM of $K_4Fe(CN)_6/K_3Fe(CN)_6$ (1:1) after each surface modification step: bare graphene,

electropolymerization of PPA (pPPA), capture antibody immobilization (CAb), blocking with BSA and incubation with enzyme-tagged cortisol (cortisol-HRP).
(G) Amperometric signals of the flexible graphene-based biosensors for 0.0–10.0 ng/mL cortisol in 0.01 M PBST, pH 7.4.
(H) Sensor performance of laser-induced graphene electrode (LGE) vs. screen printed carbon electrode (SPCEs) and glassy carbon electrodes (GCEs). Current densities were obtained from 0.0, 1.0, and 5.0 ng/mL cortisol solutions. Data are presented as mean ± standard deviation (SD) ($n = 3$).
(I) Full sigmoidal calibration curves constructed for cortisol in buffer, sweat and saliva. The sweat and saliva samples were collected from a healthy subject. Data are presented as mean ± SD ($n = 3$).
(J) Amperometric responses and percentage competition observed for 0.0 and 5.0 ng/mL cortisol with 30-second, 1-, 5-, 15-, and 60-minute incubation. Data are presented as mean ± SD ($n = 3$). (K) Validation of the flexible graphene-based biosensors toward cortisol monitoring in real samples with enzyme-linked immunosorbent assay (ELISA).

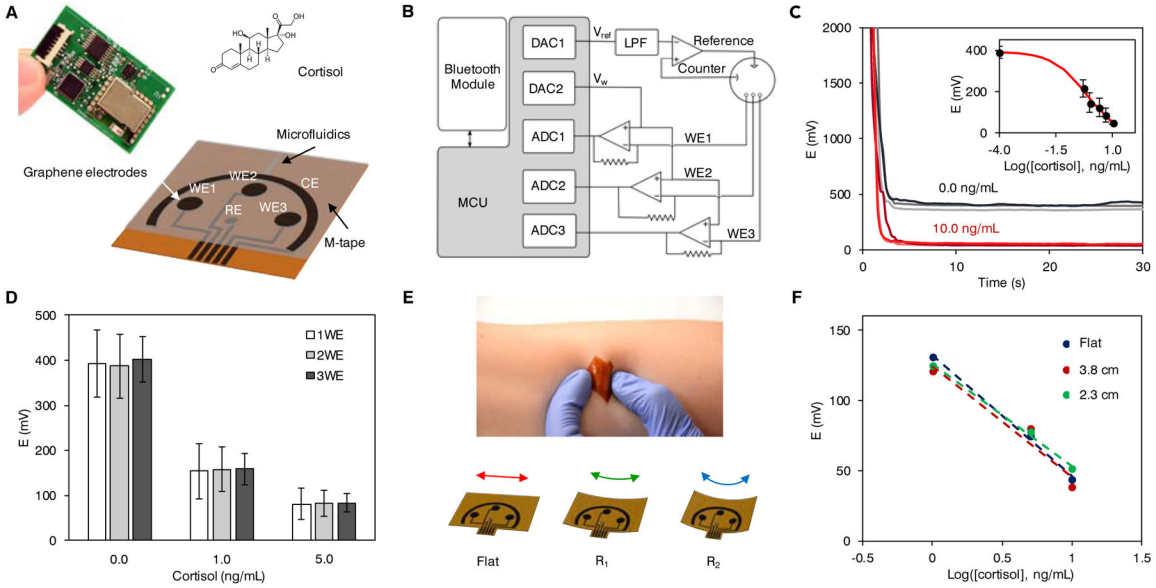

Figure 3. System integration and validation of the GS^4 toward personalized on-body use.

(A) Design of the flexible microfluidic three-working electrode (3WE) sensor array for cortisol detection and photograph of the printed circuit board (PCB) with the graphene sensor patch for signal processing and wireless communication. WE, working electrode; CE, counter electrode; RE, reference electrode.

(B) Block diagram of the GS^4. MCU, microcontroller unit; LPF, low pass filter; DAC, digital-to-analog converter; ADC, analog-to-digital converter.

(C) Sensor readings obtained wirelessly with the GS^4. Data from inset are presented as mean ± SD (n = 3).

(D) Comparison of average signals and standard deviations obtained with 1, 2, and 3 working electrodes. Data are presented as mean ± SD (n = 8).

(E) The flexible microfluidic graphene sensor array on the skin and under mechanical deformations.

(F) The responses of the sensor arrays with cortisol recognition under mechanical deformation (with radii of bending curvatures of 2.3 and 3.8 cm in 1.0, 5.0, and 10.0 ng/mL cortisol).

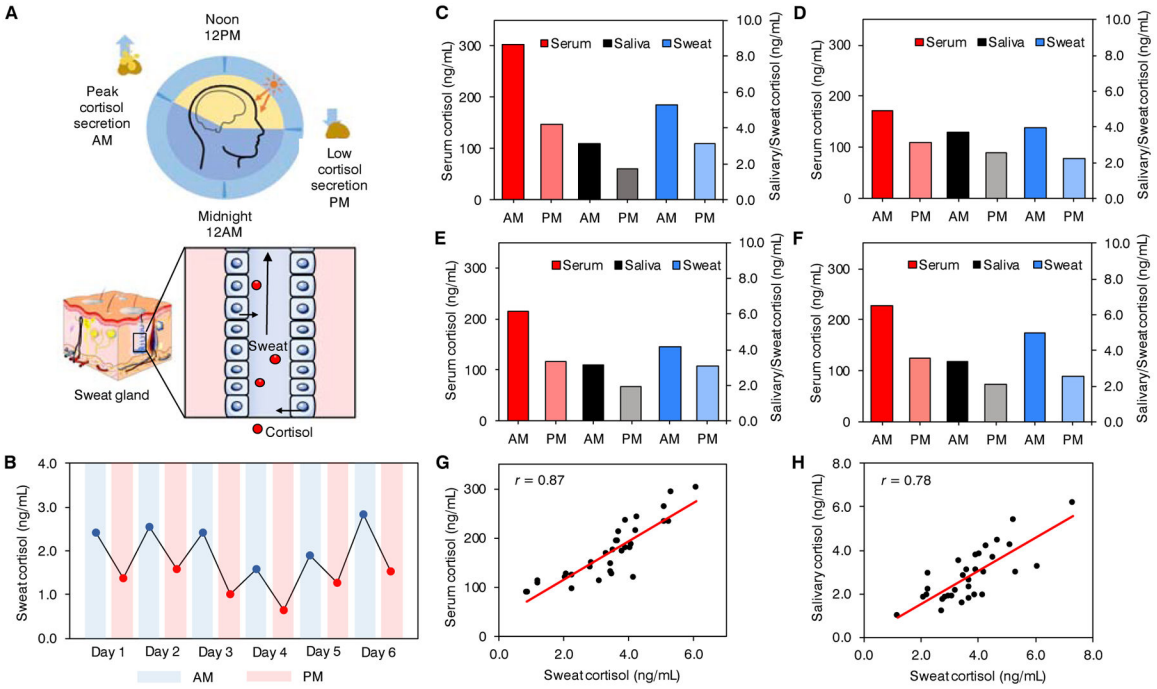

Figure 4. Investigation of the circadian rhythm of sweat stress hormone using the GS[4].

(A) Conceptual illustration of the light/dark-cycle regulated cortisol circadian rhythm and the transport of circulating cortisol to sweat.

(B) Circadian rhythm of sweat cortisol constructed for a healthy subject in a period of 6 days. Sweat was sampled and analyzed in the morning (AM) and in the afternoon (PM) each day. (C-F) Cortisol levels found in serum, saliva and sweat sampled in the AM and in the PM from four healthy subjects.

(G) Correlation of serum cortisol to sweat cortisol. The correlation coefficient *r* was acquired through Pearson's correlation analysis (eight subjects, n = 4 for each subject, $p < 0.001$).

(H) Correlation of salivary cortisol to sweat cortisol. The correlation coefficient *r* was acquired through Pearson's correlation analysis (eight subjects, n = 4 for each subject, $p < 0.001$).

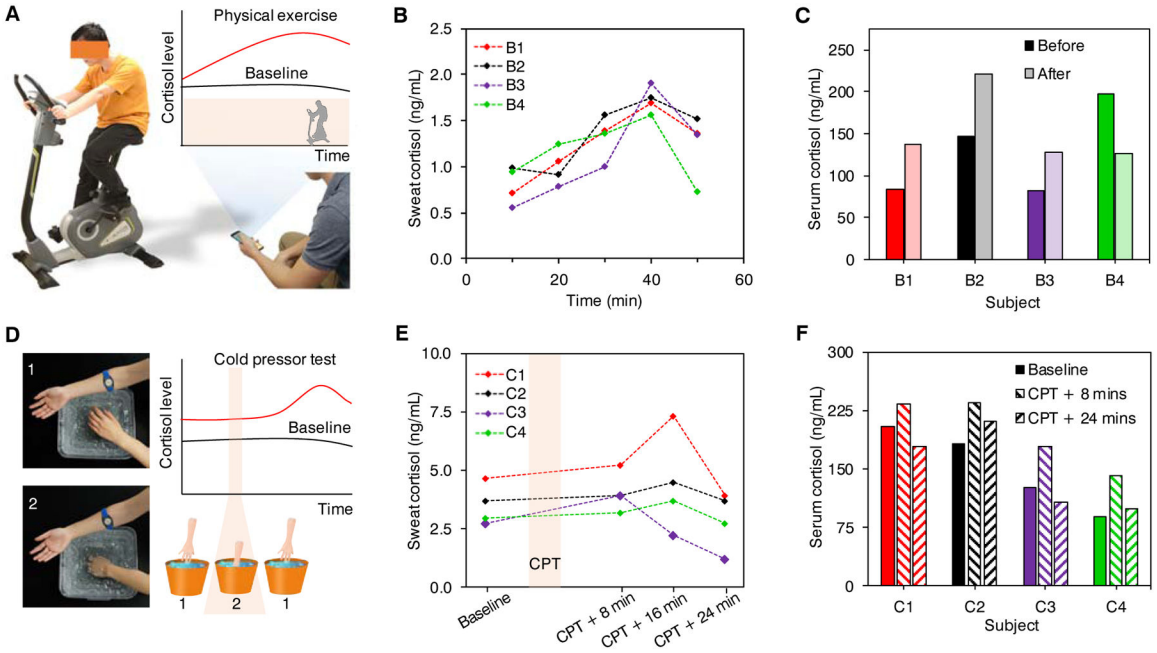

Figure 5. Dynamic monitoring of stress response using the GS[4].

(A) Conceptual illustration of stress response monitoring by tracking of a subject's cortisol level with data wirelessly transmitted to a cell phone via Bluetooth. Physical exercise is utilized as a stressor.

(B) Cortisol monitoring from three physically untrained subjects (B1-B3) and one trained subject (B4) in a constant load cycling exercise.

(C) Cortisol levels in serum sampled and analyzed before and after the cycling exercise for four subjects.

(D) Illustration of stress response in relation to the timeframe of cold pressor test (CPT) performed. (E) Cortisol monitoring from four subjects (C1-C4) undergoing CPT. Dynamic cortisol response was evaluated with iontophoresis sweat from forearm sampled and analyzed at 10-minute intervals.

(F) Cortisol levels in serum sampled before, 8 minutes after, and at the end of the CPT experiment.